Available online at www.sciencedirect.com
SCIENCE DIRECT®
C. R. Chimie 8 (2005) 541–547
COMPTES RENDUS CHIMIE
http://france.elsevier.com/direct/CRAS2C/

Full paper / Mémoire

Solvothermal synthesis, structure and Mössbauer spectroscopy of a new mixed-valence iron aluminophosphate $[Fe^{II}(H_2O)_2\ Fe_{0.8}{}^{III}Al_{1.2}(PO_4)_3]\cdot H_3O$

Li Peng, Jiyang Li *, Jihong Yu *, Guanghua Li, Qianrong Fang, Ruren Xu *

State Key Laboratory of Inorganic Synthesis and Preparative Chemistry, College of Chemistry, Jilin University, Changchun 130012, China

Received 19 May 2004; accepted 20 October 2004

Available online 12 February 2005

Abstract

A new mixed-valence open-framework iron aluminumphosphate $[Fe^{II}(H_2O)_2Fe_{0.8}{}^{III}Al_{1.2}(PO_4)_3]\cdot H_3O$ (**I**) has been synthesized under solvothermal conditions and characterized by single-crystal X-ray diffraction, compositional analyses, TG-TDA and ^{57}Fe powder absorption Mössbauer spectroscopy. Compound **I** crystallizes in the monoclinic space group *C2/c* (No. 15) with $a = 13.3200(14)$ Å, $b = 10.2104(11)$ Å, $c = 8.8412(9)$ Å, $\beta = 108.590(2)$, and $Z = 4$ with $R_1 = 0.0525$ ($I > 2\ \sigma(I)$). Its open-framework structure is built up from distorted $Fe^{II}O_4(H_2O)_2$ octahedra, $AlO_5/Fe^{III}O_5$ trigonal dipyramids and PO_4 tetrahedra, which possesses 8-memebered ring (MR) channels along [001] direction. ***To cite this article: L. Peng et al., C. R. Chimie 8 (2005).***

Résumé

Un nouvel aluminophosphate de fer microporeux à valence mixte $[Fe^{II}(H_2O)_2Fe_{0.8}{}^{III}Al_{1.2}(PO_4)_3]\cdot H_3O$ (**I**) a été synthétisé par voie solvothermale et caractérisé par diffraction de rayons X sur monocristal, analyses chimiques, analyses thermiques (TG, ATD) et spectroscopie Mössbauer du ^{57}Fe. Le composé **I** cristallise dans le groupe d'espace monoclinique *C2/c* (n° 15), avec $a = 13{,}3200(14)$ Å, $b = 10{,}2104(11)$ Å, $c = 8{,}8412(9)$ Å, $\beta = 108.590(2)°$ et $Z = 4$, avec $R_1 = 0.0525$ ($I > 2\ \sigma(I)$). Sa charpente minérale ouverte est construite à partir d'octaèdres distordus $Fe^{II}O_4(H_2O)_2$, de bipyramides trigonales $AlO_5/Fe^{III}O_5$ et de tétraèdres PO_4. Cette charpente présente des canaux parallèles à la direction [001], dont les ouvertures sont délimitées par des cycles à huit côtés. ***Pour citer cet article : L. Peng et al., C. R. Chimie 8 (2005).***

Keywords: Iron aluminophosphate; Solvothermal synthesis; Open-framework structure; Mixed-valence

Mots clés : Aluminophosphate de fer ; Synthèse solvothermale ; Charpente minérale ouverte ; Valence mixte

* Corresponding authors.
E-mail address: lijiyang@mail.jlu.edu.cn (J. Li).

1631-0748/$ - see front matter © 2005 Académie des sciences. Published by Elsevier SAS. All rights reserved.
doi:10.1016/j.crci.2004.10.027

1. Introduction

Inorganic open-framework materials with regular pore architectures are an important class of functional materials because of their widespread applications in catalysis, separation, and host–guest assemblies [1–3]. In the early 1980s, a new class of zeolite-like molecular sieves (denoted AlPOs) was first discovered by Wilson et al. [4]. Since then, a large number of aluminophosphates with rich variety of structures have been synthesized in the presence of organic amines as templates or structure directing agents. Most of these compounds have neutral open-frameworks with Al/P ration of 1, whose structures are constructed from strict alternation of AlO_4 and PO_4 tetrahedra. A variety of metal or transition metal ions can be incorporated into the frameworks of AlPOs through substituting part of Al sites to form many metal aluminophosphates (MeAPOs) with unusual catalytically activities and Brönsted acid sites [5]. Among the MeAPOs, iron-substituted aluminophosphates (FAPOs) have received considerable interest due to their magnetism characters and efficient chemical activities for some specific catalytic reactions (i.e. cyclohexane oxidation) [6,7].

Al atoms in the structures of AlPOs and MeAPOs are often found in a tetrahedral coordination, and a few can be mixed-bonded adopting four, five, and/or six coordinations with oxygen atoms as in the cases of $AlPO_4$-12 [8], $AlPO_4$-21 [9], $AlPO_4$-17 [10] and $AlPO_4$-CJ2 [11]. That all Al atoms are five-coordinated has been reported in only two compounds $K[Ni(H_2O)_2 A1_2(PO_4)_3]$ [12] and $NH_4[Co(H_2O)_2A1_2(PO_4)_3]$ [13]. In FAPO structures, the oxidation state of Fe atoms are observed as +3, +2 or mixed valences [6,7,14–18], but these atoms are often in the same coordination environments. Up to now, the metal aluminophosphates contain mixed-valence irons with different coordination states have not been reported.

Here, we describe the crystal structure of a novel iron aluminophosphate $[Fe^{II}(H_2O)_2Fe_{0.8}{}^{III}Al_{1.2}(PO_4)_3]\cdot H_3O$ (**I**). Its structure is closely related to that of nickel aluminophosphate $K[Ni(H_2O)_2A1_2(PO_4)_3]$ and cobalt aluminophosphate $NH_4[Co(H_2O)_2A1_2(PO_4)_3]$. However, the mixed-valence iron atoms (Fe^{II}/Fe^{III} in the ratio of 5/4) and their particular coordination environments in **I** make it interesting from both structure and property point of view.

2. Experimental section

2.1. Synthesis

The synthesis of **I** was carried out using solvothermal method in a gel with molar composition 1.0 $(i\text{-PrO})_3Al$: 0.5 $FeCl_2\cdot 4\ H_2O$: 4.1 H_3PO_4: 4.8 imidazole: 12.0 triethylene glycol (TEG). The typical synthesis procedure was as follows: 2.0 g of $(i\text{-PrO})_3Al$ was first dispersed into 16 ml of TEG with stirring, 3.2 g of imidazole and 2.72 ml of phosphoric acid (H_3PO_4, 85% in water) was then added, the mixture was stirred until it was homogeneous. Finally, 0.97 g of $FeCl_2\cdot 4H_2O$ was added to the above reaction mixture. The reaction mixture was further stirred for 1 h, and then was sealed in a Teflon-lined stainless steel autoclaves and heated in an oven at 180 °C for 5 days under static conditions. Deep purple-red rhombus crystals of **I** crystallized in a yield of 15% based on iron together with light khaki byproducts (an iron–aluminum phosphate with LAU structure type). A batch of crystals of **I** were carefully separated under the optical microscope for the further analysis.

2.2. Compositional analyses

Inductively coupled plasma (ICP) analysis was performed on a Perkin–Elmer Optima 3300 DV ICP instrument, which gave the contents of Al as 6.93 wt.%, Fe as 20.95 wt.% and P as 20.57 wt.% (calcd Al: 6.85; Fe: 21.32; P 19.67). Elemental analyses conducted on a Perkin–Elmer 2400 elemental analyzer indicated that no organic molecules or NH_4^+ ions were occluded in **I**.

2.3. Thermal analysis

TG-DTA measurements were obtained using a NETZSCH STA 449C unit with a heating rate of 10 °C/min under air atmosphere up to 800 °C. As shown in Fig. 1, the thermogravimetric analysis gave one step weight loss of 12.5 wt.% (calcd 11.6 wt.%) from 350 to 500 °C, which corresponded to the remove of water molecules in **I**. The further XRD analysis indicated that the structure of **I** was collapsed and transformed to dense phase after it calcinated at 400 °C for 2 h to remove water. The ^{57}Fe Mössbauer Spectrometry of the calcined sample showed that all of the iron atoms are Fe(III).

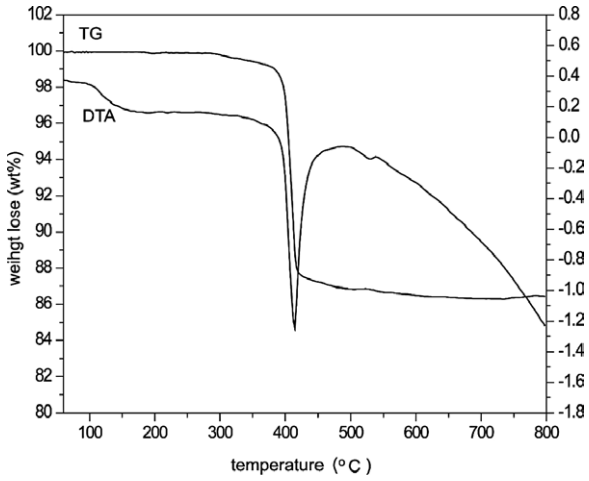

Fig. 1. TG-DTA curve of **I**.

2.4. Single-crystal X-ray diffraction analysis

A suitable single crystal with dimensions of 0.15 × 0.15 × v0.03 mm^3 was carefully selected and glued onto a glass fiber for single-crystal X-ray diffraction analysis. The intensive data were collected on a Siemens SMART CCD diffractometer using graphite-monochromated Mo Kα radiation (λ = 0.71073 Å) at a temperature of 20 ± 2 °C. Data processing was accomplished with the SAINT processing program [19]. The structure was solved in the space group *C2/c* by direct methods and refined by a full-matrix least-squares approach on F^2 by SHELXTL software package [20]. The partial occupancy of aluminum by iron on the site of five-coordinated atom was not considered at first. A full occupancy of the aluminum on this site led the thermal parameter to zero, while a full occupancy of iron on this site led to the thermal parameters of others atoms converging to zero. Then the occupancy factor of this site was refined and converged to a ratio close to 60:40 for Al/Fe in order to be in agreement with the chemical analysis (Al/Fe ratio of 2/3) of **I**. Crystal data and details of the data collection are listed in Table 1. Table 2 presents the final atomic coordinates and isotropic thermal parameters. The selected bond lengths and bond angles are listed in Table 3.

2.5. ^{57}Fe Mössbauer spectrometry

The ^{57}Fe powder absorption Mössbauer spectra were recorded by a conventional constant acceleration Mössbauer spectrometer with a ^{57}Co/Pd source at room temperature. All isomer shift values (*d*) given hereafter were

Table 1
Crystal data and structure refinement for compound **I**

Empirical formula	H7 Al1.20 Fe1.80 O15 P3
Formula weight	472.87
Temperature	293(2) K
Wavelength	0.71073 Å
Crystal system, space group	Monoclinic, *C2/c*
Unit cell dimensions	a = 13.3200(14) Å α = 90°
	b = 10.2104(11) Å β = 108.590(2)°
	c = 8.8412(9) Å γ = 90(3)
Volume	2436.97(11) Å^3
Z, Calculated density	4, 2.756 Mg/m^3
Absorption coefficient	2.906 per mm
F(000)	938
Crystal size (mm)	0.15 × 0.15 × 0.03
Theta range for data collection	2.57–28.18°
Limiting indices	$-17 \le h \le 13$, $-13 \le k \le 12$, $-11 \le l \le 11$
Reflections collected/unique	3422/1306 [*R*(int) = 0.0352]
Completeness to theta = 28.18	93.4%
Refinement method	Full-matrix least-squares on F^2
Data/restraints/parameters	1306/1/104
Goodness-of-fit on F^2	1.174
Final *R* indices [$I > 2\sigma(I)$]	R_1 = 0.0525, wR_2 = 0.1155
R indices (all data)	R_1 = 0.0611, wR_2 = 0.1186
Largest diff. peak and hole	0.839 and –0.555 e/Å^3

* $R_1 = \Sigma(\Delta F/\Sigma(F_o))$; $wR_2 = (\Sigma[w(F_o^2-F_c^2)])/\Sigma[w(F_o^2)^2]^{1/2}$, $w = 1/\sigma^2(F_o^2)$.

Table 2
Atomic coordinates (× 10^4) and equivalent isotropic displacement parameters (Å^2 × 10^3) for compound **I**

	x	*y*	*z*	*U*(eq)
Fe(1)[a]	0	–2124(1)	–2500	12(1)
Fe(2)[b]	–1703(1)	–4241(1)	–742(1)	12(1)
Al(1)[c]	–1703(1)	–4241(1)	–742(1)	12(1)
P(1)	0	–4940(2)	–2500 8(1)	
P(2)	–2907(1)	–6258(1)	3297(2)	10(1)
O(1)	–717(3)	–4001(3)	1955(4)	12(1)
O(2)	–2092(3)	–5817(3)	1704(4)	13(1)
O(3)	–610(3)	–4166(4)	1133(4)	13(1)
O(4)	–2327(3)	–2716(3)	–1571(4)	14(1)
O(5)	–2728(3)	–4510(3)	324(4)	13(1)
O(6)	–971(3)	–1016(4)	–1694(5)	18(1)
O(7)	1136(4)	–1983(5)	–128(6)	25(1)
O(1W)	0	1376(8)	–2500	57(2)

[a] *U*(eq) is defined as one third of the trace of the orthogonalized Uij tensor.
[b] Occupancy factor fixed at 40%.
[c] Occupancy factor fixed at 60%.

referred to as α-iron. Experimental data were resolved into symmetric quadrupole doublets with Lorentzian lineshapes using an iterative least-square fit program.

3. Results and discussion

3.1. Structure description

Each asymmetric unit of **I,** as shown in Fig. 2, contains 12 crystallographically independent non-hydrogen atoms including 1 Fe, 1 M with Al/Fe ratio of 3/2, 2 P and 8 O atoms. Fe(1) is six-coordinated on the twofold axis, which is linked to two equivalent PO_4 tetrahedra via two bridging O(6) atoms (Fe(1)–O(6) = 2.012(4) Å) and two H_2O molecules (Fe(1)–OH_2 = 2.165(5) Å) in a *trans*-position. The remaining two vertices are two μ_3-O atoms (Fe(1)–O(1) = 2.260(4) Å) that are bonded to two AlO_5 trigonal bipyramids and a PO_4 tetrahedra sharing one edge with Fe(1). The O–Fe–O bond angles are in the range of 64.08–172.4°, indicating the $FeO_4(H_2O)_2$ octahedron is highly distorted. Bond-valence calculation [21] results suggest that the Fe(1) is present as Fe^{2+}. M is five-coordinated to four bridging oxygen and one μ_3-O atom, making five M–O–P bonds and one M–O–Fe bond. The M–O bond length (1.806(4)–1.957(3) Å) is clearly longer than the Al–O distances (1.770–1.927 Å) in the related structures of $K[Ni(H_2O)_2Al_2(PO_4)_3]$ [12] and

Table 3
Selected bond lengths (Å) and angles (°) for compound **I**

Fe(1)–O(6)#1	2.012(4)
Fe(1)–O(6)	2.012(4)
Fe(1)–O(7)#	12.165(5)
Fe(1)–O(7)	2.165(5)
Fe(1)–O(1)	2.260(4)
Fe(1)–O(1)#	12.260(4)
M–O(4)	1.806(4)
M–O(2)	1.817(4)
M–O(3)	1.825(4)
M–O(5)	1.910(4)
M–O(1)	1.957(3)
P(1)–O(3)#2	1.526(4)
P(1)–O(3)#3	1.526(4)
P(1)–O(1)	1.535(4)
P(1)–O(1)#1	1.535(4)
P(2)–O(6)#4	1.513(4)
P(2)–O(5)#2	1.531(4)
P(2)–O(4)#4	1.533(4)
P(2)–O(2)	1.546(4)
O(7)–H(7A)...O(2)#3	2.824(6)
O(7)–H(7B)...O(5)#7	2.905(6)
O(6)#1–Fe(1)–O(6)	111.6(2)
O(6)#1–Fe(1)–O(7)#1	87.09(17)
O(6)–Fe(1)–O(7)#1	88.62(17)
O(6)#1–Fe(1)–O(7)	88.62(17)
O(6)–Fe(1)–O(7)	87.09(17)
O(7)#1–Fe(1)–O(7)	172.4(3)
O(6)#1–Fe(1)–O(1)	156.23(14)
O(6)–Fe(1)–O(1)	92.18(14)
O(7)#1–Fe(1)–O(1)	92.90(16)
O(7)–Fe(1)–O(1)	93.57(15)
O(6)#1–Fe(1)–O(1)#1	92.18(14)
O(6)–Fe(1)–O(1)#1	156.23(14)
O(7)#1–Fe(1)–O(1)#1	93.57(15)
O(7)–Fe(1)–O(1)#1	92.90(16)
O(1)–Fe(1)–O(1)#1	64.08(17)
O(4)–M–O(2)	123.21(17)
O(4)–M–O(3)	117.57(17)
O(2)–M–O(3)	119.21(17)
O(4)–M–O(5)	90.90(16)
O(2)–M–O(5)	87.75(16)
O(3)–M–O(5)	92.67(16)
O(4)–M–O(1)	88.40(15)
O(2)–M–O(1)	89.74(16)
O(3)–M–O(1)	90.71(16)
O(5)–M–O(1)	176.48(16)
O(3)#2–P(1)–O(3)#3	106.5(3)
O(3)#2–P(1)–O(1)	113.24(18)
O(3)#3–P(1)–O(1)	110.64(19)
O(3)#2–P(1)–O(1)#1	110.64(19)

(continued on next page)

Table 3
(continued)

O(3)#3–P(1)–O(1)#1	113.24(18)
O(1)–P(1)–O(1)#1	102.7(3)
O(6)#4–P(2)–O(5)#2	108.5(2)
O(6)#4–P(2)–O(4)#4	112.5(2)
O(5)#2–P(2)–O(4)#4	110.5(2)
O(6)#4–P(2)–O(2)	111.3(2)
O(5)#2–P(2)–O(2)	109.5(2)
O(4)#4–P(2)–O(2)	104.6(2)
P(1)–O(1)–M	133.4(2)
P(1)–O(1)–Fe(1)	96.59(17)
M–O(1)–Fe(1)	128.73(17)
P(2)–O(2)–M	134.2(2)
P(1)#3–O(3)–M	139.7(2)
P(2)#5–O(4)–M	142.1(2)
P(2)#6–O(5)–M	129.5(2)
P(2)#5–O(6)–Fe(1)	130.7(2)

Symmetry transformations used to generate equivalent atoms: #1 –*x*, *y*, –*z* – 1/2 #2 *x*, –*y* – 1, *z* – 1/2 #3 –*x*, –*y* – 1, –*z* #4 –*x* – 1/2, *y* – 1/2, –*z* – 1/2; #5 –*x* – 1/2, *y* + 1/2, –*z* – 1/2 #6 *x*, –*y* – 1, *z* + 1/2 #7 *x* + 1/2, *y* + 1/2, *z*.

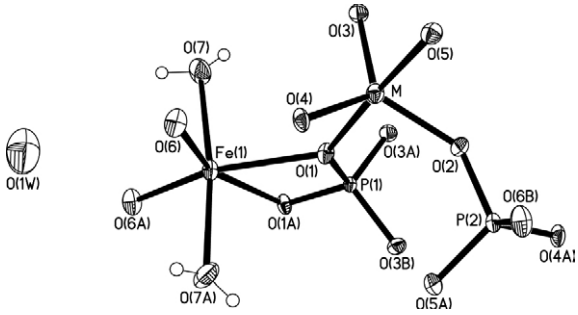

Fig. 2. Thermal ellipsoid plot (50% probability) and atomic labeling scheme of **I**.

$NH_4[Co(H_2O)_2Al_2(PO_4)_3]$ [13]. This is caused by 40% of Al substituted by Fe on this position based on the ICP analysis. Both two distinct P atoms with of P(1) on the twofold axis are tetrahedrally coordinated by oxygen atoms connecting to M and Fe atoms. The P–O bond lengths (1.513(4)–1.546(4) Å) and O–P–O bond angles (102.7(3)–113.24(18)°) are within the expected ranges.

The linkages of $FeO_4(H_2O)_2$ octahedra, MO_5 trigonal bipyramids and PO_4 tetrahedra through oxygen form the open-framework of **I**, which contains 8-membered

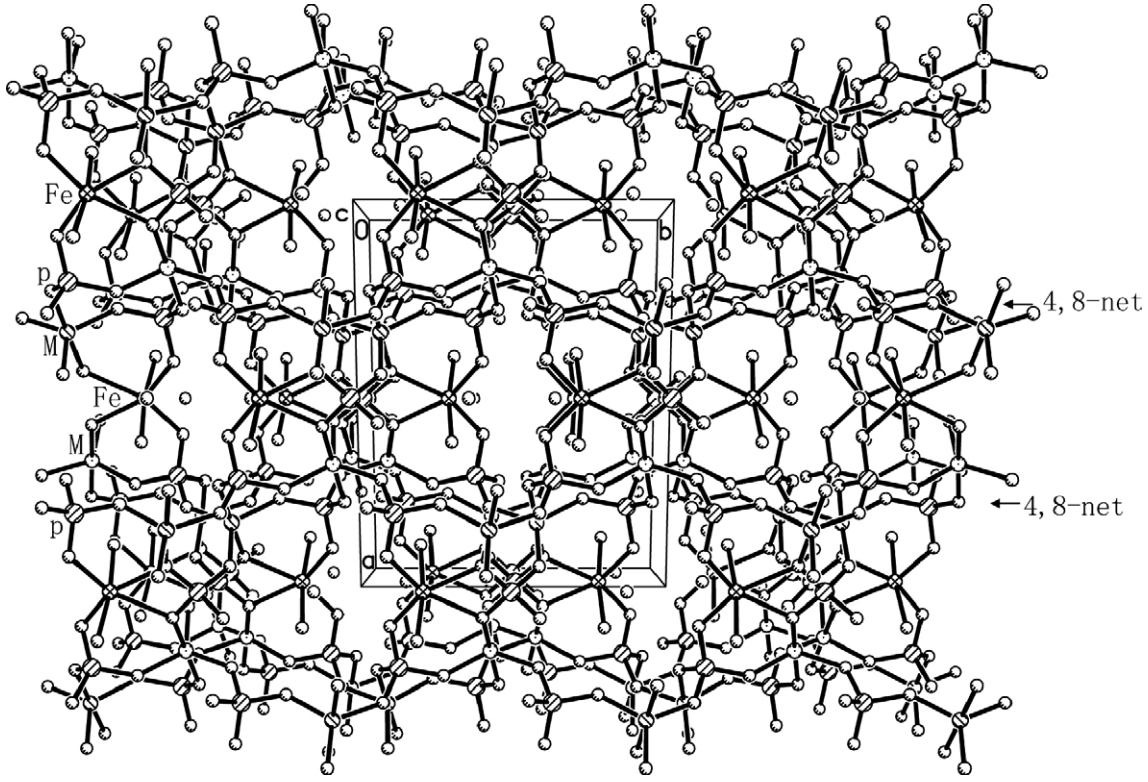

Fig. 3. Projected view of the framework of **I** along the [001] direction shows the 8-MR channels and water locations.

ring (MR) channels along the [001] direction (Fig. 3). It consists of anionic framework of formula $[Fe^{II}(H_2O)_2Fe^{III}_{0.8}Al_{1.2}(PO_4)_3]^-$, whose negative charges are compensated by the protonated H_3O^+. Considering the charge neutrality of **I**, the five-coordinated Fe should has an oxidation state of +3. This is further confirmed by the Mössbauer study as discussed below. The anionic framework of **I** is similar to those of nickel aluminophosphate $K[Ni(H_2O)_2Al_2(PO_4)_3]$ and cobalt aluminophosphate $NH_4[Co(H_2O)_2Al_2(PO_4)_3]$. Its framework can be described as a series of 2D 4,8-net sheets (Fig. 4) formed by alternating MO_5 trigonal bipyramids and PO_4 tetrahedra, which are further connected together by P(1) and $Fe^{II}(1)$ coordinated two H_2O molecules. One protonated H_3O^+ molecule locates in each 8-MR channel (Fig. 3) and forms 2 weak H-bonds with the oxygen atoms in the framework. The H-bonding distances are 2.824(6) Å for O(7)–H(7A)···O(2) and 2.905(6)Å for O(7)–H(7B)···O(5).

3.2. *^{57}Fe Mössbauer spectrometry*

^{57}Fe Mössbauer spectroscopy can help to determine whether iron atoms are Fe(II), Fe(III) [22–25] or mixed-valence [26–35]. The room-temperature Mössbauer powder spectrum of the sample (Fig. 5) indicates the presence of pure electric quadrupole interactions, and the spectrum was fitted by means of classical symmetric Lorentzian doublets. The fit obtained from a decomposition of the spectrum can be divided into two doublets (as seen in Table 4). The isomer shift and quadrupole splitting for narrow one are 0.33 and 0.34 mm/s, respectively, which are typical for high-spin trivalent iron. While the value for the wide one is corresponded to high-spin divalent iron [36]. Furthermore, the observed relative intensities of two doublets lead to Fe^{3+}/Fe^{2+} ratio of 44.65/55.35, closed to 4/5.

Up to now, three transitional metal elements Fe, Co and Ni have been successfully incorporated into this kind of octahedron–trigonal bipyramid–tetrahedra framework. The iron substituted case is particularly interesting because it contains the mixed-valence Fe(II) and Fe(III) atoms. The formation of Fe(II)–O–Fe(III) bond and the unusual coordination environments of iron atoms will cause the interesting magnetic and electronic properties of **I**. Further work is under going.

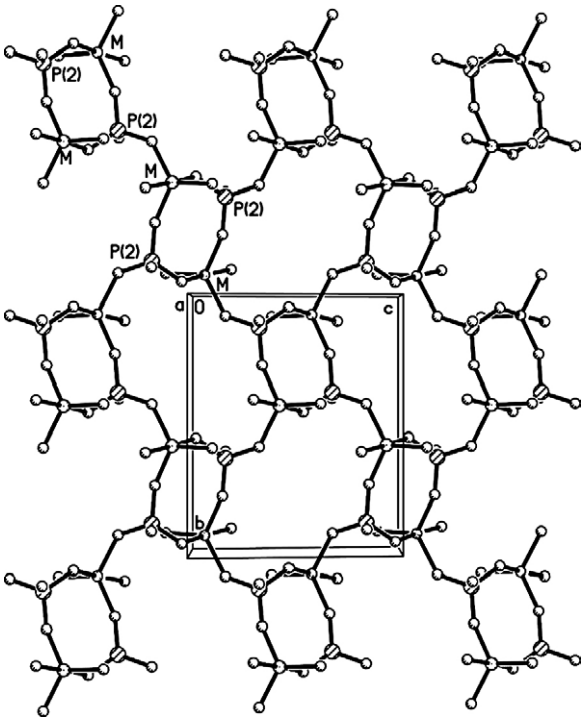

Fig. 4. The 4,8-net sheet.

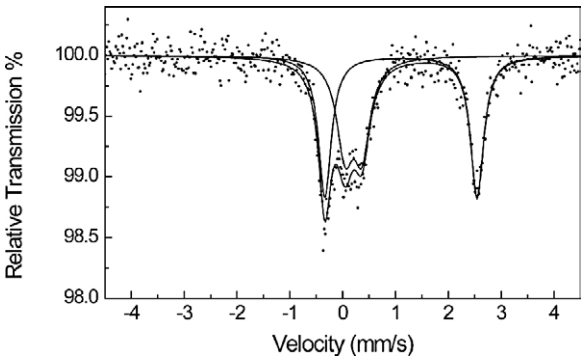

Fig. 5. Mössbauer spectra of **I** at room temperature.

Table 4
Mössbauer parameters for compound **I**

Subspectrum	IS (mm/s)	QS (mm/s)	W (mm/s)	Rel. area (%)
Narrow doublet	0.33	0.34	0.21	44.65
Wide doublet	1.24	2.89	0.17	55.35

IS: isomeric shifts; QS: quadrupole splitting; W: full width at half maximum. The errors of the hyperfine parameters are about 1% and of the relative areas 5%.

5. Acknowledgments

We are grateful to the National Natural Science Foundation of China and the State Basic Research Project (G2000077507) for financial supports.

The supplementary material has been sent to the Fachinformationzentrum Karisruhe, Abt. PROKA, 76344 Eggenstein-Leopoldshafen, Germany, as supplementary material CSD-number 414052 and can be obtained by contacting the FIZ.

References

[1] M.E. Davis, Nature 417 (2002) 813.
[2] M.E. Davis, R.F. Lobo, Chem. Mater. 4 (1992) 756.
[3] A. Corma, Chem. Rev. 95 (1995) 559.
[4] S.T. Wilson, B.M. Lok, C.A. Messina, T.R. Carman, E.M, Flanigen, J. Am. Chem. Soc. 104 (1982) 1146.
[5] M. Hartmann, L. Kevan, Chem. Rev. 99 (1999) 635.
[6] R. Raja, G. Sankar, J.M. Thomas, J. Am. Chem. Soc. 121 (1999) 11926.
[7] M. Dugal, G. Sankar, R. Raja, J.M. Thomas, Angew. Chem. Int. Ed. Engl. 39 (2000) 2310.
[8] J.B. Parise, Inorg. Chem. 24 (1985) 4312.
[9] J.B. Parise, Acta. Crystallogr. Sect. C 41 (1984) 515.
[10] J.J. Pluth, J.V. Smith, J.M. Bennett, Acta. Crystallogr. Sect. C 42 (1986) 283.
[11] G. Férey, T. Loiseau, P. Lacorre, F. Taulelle, J. Solid-State Chem. 105 (1993) 179.
[12] L.M. Meyer, R.C. Haushalter, Chem. Mater. 6 (1994) 349.
[13] C. Panz, K. Polborn, P. Behrens, Inorg. Chim. Acta 269 (1998) 73.
[14] C.M. Cardile, N.J. Tapp, N.B. Milestone, Zeolites 10 (1990) 90.
[15] P.-S. Dai, R.H. Petty, C.W. Ingram, R. Szostak, Appl. Catal. A 143 (1996) 101.
[16] A. Ristić, N.N. Tušar, I. Arčon, F. Thibault-Starzyk, D. Hanžel, J. Czyzniewska, V. Kaučič, Micropor. Mesopor. Mater. 56 (2002) 303.
[17] K. Lázár, A.J. Chandwadkar, P. Fejes, J. Čejka, A.V. Ramaswamy, J. Radioanal. Nucl. Chem. 246 (2000) 143.
[18] L. Beitone, T. Loiseau, F. Millange, C. Huguenard, G. Fink, F. Taulelle, J.-M. Grenèche, G. Férey, Chem. Mater. 15 (2003) 4590.
[19] SMART and SAINT software packages, Siemens Analytical X-ray Instruments, Inc.: Madison, WI, 1996.
[20] G.M. Sheldrick, SHELXTL-NT, Version 5.1, Brucker AXS, Madison, WI, 1997.
[21] N.E. Brese, M. O'Keefe, Acta. Crystallogr. B47 (1991) 192.
[22] P. Gütlich, A. Hauser, H. Spiering, Angew. Chem. Int. Ed. Engl. 33 (1994) 2024.
[23] J. Zarembowitch, New J. Chem. 16 (1992) 255.
[24] P. Gütlich, A. Hauser, Coord. Chem. Rev. 97 (1990) 1.
[25] H. Toftlund, Coord. Chem. Rev. 94 (1989) 67.
[26] B. Kersting, M.J. Kolm, C. Janiak, Z. Anorg, Allg. Chem. 624 (1998) 775.
[27] B. Kersting, D. Siebert, D. Volkmer, M.J. Kolm, C. Janiak, Inorg. Chem. 38 (1999) 3871.
[28] A. Geiss, M.J. Kolm, C. Janiak, H. Vahrenkamp, Inorg. Chem. 39 (2000) 4037.
[29] T. Manago, S. Hayami, H. Oshio, S. Osaki, H. Hasuyama, R.H. Herber, Y. Maeda, J. Chem. Soc., Dalton Trans. 6 (1999) 1001.
[30] J.R.D. DeBord, W.M. Reiff, C.J. Warren, R.C. Haushalter, J. Zubieta, Chem. Mater. 9 (1997) 1994.
[31] D. Lee, J.L. DuBois, B. Pierce, B. Hedman, K.O. Hodgson, M.P. Hendrich, S.J. Lippard, Inorg. Chem. 41 (2002) 3172.
[32] W.E. Buschmann, J. Ensling, P. Gütlich, J.S. Miller, Chem. Eur. J. 5 (1999) 3019.
[33] M. Sato, Y. Hayashi, T. Tsuda, M. Katada, Inorg. Chim. Acta 261 (1997) 113.
[34] C.-C. Wu, H.G. Jang, A.L. Rheingold, P. Gütlich, D.N. Hendrickson, Inorg. Chem. 35 (1996) 4137.
[35] A.-S. Khalid, W. Heiner, G. Michael, E. Franziska, W. Biao, J. Christoph, J. Chem. Soc., Dalton Trans. 14 (2003) 2815.
[36] N.N. Greenwood, T.C. Gibb, Mössbauer Spectroscopy, Chapman and Hall, London, 1971.